Supplementary material for *Energy and dissipation spectra of waves propagating in the inner surf zone*

P. Bonneton

October 17, 2023

UMR 5805 EPOC, CNRS - University of Bordeaux, Allée Geoffroy Saint-Hilaire, F-33615 Pessac, France

A Burgers' spectra

A.1 Periodic sawtooth waves

In the non-diffusive case ($\nu = 0$), the periodic SW Burgers solution, $v_i(x,t)$, is given by

$$v_i = \frac{V_J(t)}{2}\left(\frac{2x}{\lambda} - \mathrm{sgn}(x)\right) \qquad x \in [-\frac{\lambda}{2}, \frac{\lambda}{2}] \quad , \tag{1}$$

where λ is the wavelength, $V_J(t) = \frac{V_0}{1+V_0 t/\lambda}$ is the velocity jump across the inviscid shock (located in $x = 0$) and V_0 is the velocity jump at $t = 0$. Khokhlov derived an exact SW solution of the diffusive Burgers' equation (see *Gurbatov et al.* (2012))

$$v = \frac{V_J(t)}{2}\left(\frac{2x}{\lambda} - \tanh\frac{V_J(t)x}{4\nu}\right) \ . \tag{2}$$

This solution is not periodic, but for large Reynolds numbers it becomes quasi-periodic between $x = -\lambda/2$ and $x = \lambda/2$, with a diffusive front located in $x = 0$.

In figure 1 we present a comparison between the quasi-periodic theoretical solution (2) and the numerical solution of the Burgers' equation based on a Fourier spectral method. We consider the transformation of an initially sinusoidal wave field into a SW field. Figure 1 shows that there is no distinguishable difference between theoretical and numerical SW solutions.

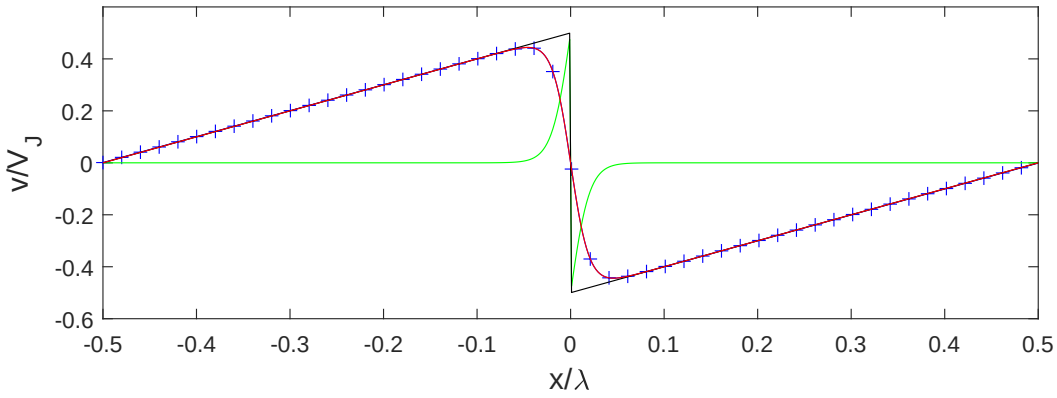

Figure 1: Profile of a periodic Burgers SW at $R_B = 200$. Red line, diffusive solution (equation 2); black line, non-diffusive solution (equation 1); green line, diffusive correction $C = \frac{V_J}{2}\left(-\mathrm{sgn}(x) + \tanh\frac{V_J x}{4\nu}\right)$; +, discrete form (every 10 points) of the numerical solution (Fourier spectral model) of the Burgers' equation at dimensionless time $U_0 t/\lambda = 4.67$ ($R_B = 200$), for a sinusoidal initial condition $v(x, t = 0) = 0.5U_0 \sin(2\pi/\lambda)$ with $R_B(t = 0) = 1000$.

We will now derive an expression for the SW energy spectrum based on the Khokhlov solution (2). Since v given by this equation is an odd function of x we can expand v as a sine series

$$v(x,t) = \sum_{n=1}^{\infty} v_n(t)\sin(nk_p x) \ ,$$

where $k_p = \frac{2\pi}{\lambda}$ and v_n is the n^{th} Fourier coefficient

$$v_n(t) = \frac{4}{\lambda}\int_0^{\lambda/2} v(x,t)\sin(nk_p x)dx \ .$$

By decomposing the velocity field into $v = v_i - C$, with C the diffusive correction given by $C = \frac{V_J}{2}\left(-\mathrm{sgn}(x) + \tanh\frac{V_J x}{4\nu}\right)$, the Fourier coefficients of

the Khokhlov solution (2) can be rewritten as

$$v_n(t) = \frac{4}{\lambda}\left(\int_0^{\lambda/2} V_J(x,t)\sin(nk_p x)dx - \int_0^{\lambda/2} C\sin(nk_p x)dx\right) .$$

As illustrated in figure 1, the diffusive correction C rapidly decreases to zero as x increases. The upper bound of the second integral can therefore be replaced by ∞. The approximate integral can then be solved by using tables of Fourier transforms (e.g., *Oberhettinger*, 1957). Finally, the Fourier coefficients can be expressed as

$$v_n(t) = -2\nu k_p \mathrm{csch}\left(\frac{2\pi\nu}{V_J} n k_p\right) ,$$

and the energy spectral density, $\mathcal{E}_{v_n} = \frac{v_n^2}{2}$, as

$$\mathcal{E}_{v_n} = 2\nu^2 k_p^2 \mathrm{csch}^2\left(\frac{k_n}{k_\nu}\right) , \tag{3}$$

where $k_n = nk_p$ and $k_\nu = \frac{V_J}{2\pi\nu}$. For $k_n/k_\nu \ll 1$, $\mathcal{E}_{v_n}$ follows a k_n^{-2} power law

$$\mathcal{E}_{v_n} = \frac{2V_J^2}{\lambda^2} k_n^{-2} . \tag{4}$$

This last relation is also the exact energy spectral density of the non-diffusive SW solution (1). In the following, the inertial and diffusive subranges will be defined respectively as $k \in [k_p, k_\nu]$ and $k \in [k_\nu, \infty]$. The dimensionless width of the inertial subrange, $(k_\nu - k_p)/k_p$, increases linearly with R_B, since $k_\nu/k_p = R_B/(4\pi^2)$.

We now present a comparison between the theoretical spectrum (3) and spectra obtained from numerical solutions of the Burgers' equation. We consider the transformation of an initially sinusoidal wave field into a SW field. As a sawtooth wave evolves, its velocity jump, and consequently, its Reynolds number decrease. Energy spectra for two Reynolds numbers ($R_B = 200$ and 400) representative of those in the ISZ are presented in figure 2. We can see that there is no distinguishable difference between the theoretical solution

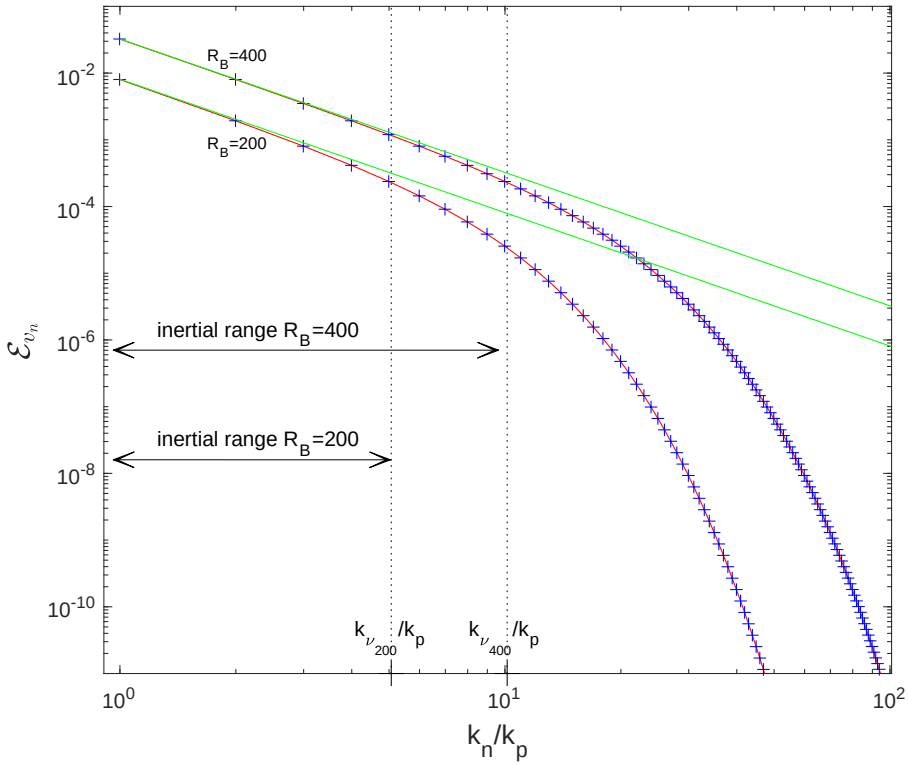

Figure 2: Energy spectral density of periodic Burgers SW at $R_B = 400$ and 200. Red line, diffusive solution (equation (3)); green line, non-diffusive solution (equation (4)); +, numerical solutions of the Burgers' equation at dimensionless times $V_0 t/\lambda = 2.17$ ($R_B = 400$) and $V_0 t/\lambda = 4.67$ ($R_B = 200$), for a sinusoidal initial condition $v(x, t = 0) = 0.5 V_0 \sin(2\pi/\lambda)$ with $R_B(t = 0) = 1000$; dotted lines, positions of k_ν/k_p. For the sake of clarity we use continuous lines to represent the discrete energy spectra (3) and (4).

(3) and the numerical one. In the inertial subrange the energy spectrum tends to follow the k_n^{-2} power law given by equation (4). The decrease with time in the inertial subrange width, associated with the decrease in R_B, is illustrated in figure 2.

A.2 Random sawtooth waves

We now consider freely decaying random solutions $v(x,t)$ which are statistically homogeneous in space with zero mean. The power spectral density $\Phi(k,t)$ is the Fourier transform of the auto-correlation function $R(r)$

$$\Phi(k,t) = \frac{1}{2\pi}\int_{-\infty}^{\infty} R(r)\exp(-ikr)dr \ , \tag{5}$$

where $R(r,t) = \langle v(x,t)v(x+r,t)\rangle$. $\Phi(k,t)$ being an even function of k, we limit our analysis to $k \geq 0$ and denote $E_v(k,t) = 2\Phi(k,t)$ the power spectral density function. With this notation, the total energy, $\mathbf{E}_v = \langle v^2\rangle = \int_{-\infty}^{\infty}\Phi(k)dk$, can be expressed as

$$\mathbf{E}_v = \int_0^{\infty} E_v(k)dk \ .$$

The assumption of isotropy implies $R(-r) = R(r)$ and then

$$E_v(k,t) = \frac{2}{\pi}\int_0^{\infty} R(r)\cos(kr)dr \ . \tag{6}$$

After two integrations by parts equation (6) can be rewritten as

$$E_v(k,t) = \frac{2}{\pi k^2}\int_0^{\infty}\frac{d^2Q}{dr^2}\cos(kr)dr \ , \tag{7}$$

where $Q(x,t) = \frac{1}{2}\langle(v(x+r,t)-v(x,t))^2\rangle$ and $R(r,t) = \langle v(x,t)^2\rangle - Q(x,t)$.

In order to estimate $E_v(k,t)$ in the SW regime, *Saffman* (1968) assumed that the periodic solution (2) reproduces the qualitative features of the small-scale behavior of random sawtooth waves. He then found that, for $r \ll \lambda_m$, $Q(r,t)$ can be estimated by

$$Q(r,t) = \frac{V_c(t)^2}{2\lambda_m(t)}\left(r\coth\left(\frac{V_c(t)}{4\nu}r\right) - \frac{4\nu}{V_c(t)}\right) \ , \tag{8}$$

where λ_m is the mean distance between adjacent wave fronts and V_c the characteristic scale of velocity jumps at wave fronts.

By substituing (8) into (7) we obtain

$$E_v(k,t) = \frac{V_c^2}{\pi\lambda_m k^2}\int_0^\infty \frac{d^2}{dr^2}\left(r\coth(\alpha r)\right)\cos(kr)dr \ ,$$

or

$$E_v(k,t) = \frac{V_c^2}{\pi\lambda_m k^2}\int_0^\infty \frac{d^2\xi}{dr^2}\cos(kr)dr \ ,$$

where $\xi(r) = r(\coth(\alpha r) - 1)$ and $\alpha = \frac{V_c}{4\nu}$. After two integrations by parts

$$E_v(k,t) = \frac{V_c^2}{\pi\lambda_m k^2}F(k) \ ,$$

where

$$F(k) = 1 - k^2\int_0^\infty \xi(r)\cos(kr)dr \ .$$

$F(k)$ can be written

$$F(k) = 1 - k^2\frac{dG}{dk} \ ,$$

where $G(k) = \int_0^\infty(\coth(\alpha r) - 1)\sin(kr)dr$.

By using tables of Fourier transforms (e.g., *Oberhettinger*, 1957) we have

$$G(k) = -k^{-1} + \frac{\pi}{2\alpha}\coth(\pi k/(2\alpha))$$

then

$$F(k) = k^2\frac{\pi^2}{4\alpha^2}\mathrm{csch}^2(\pi k/(2\alpha))$$

and finally

$$E_v(k) = 2\nu^2 k_m \mathrm{csch}^2(2\pi\nu k/V_c) \ .$$

This spectrum law differs slightly from the *Saffman* (1968) law

$$E_S(k) = \frac{2\pi\nu^2}{L}\mathrm{csch}^2(\pi\nu k/(2V_c)) \ ,$$

where Saffman defined L as the *averaged distance* between wave fronts (i.e., λ_m). We have shown that in fact $L = \lambda_m/2$. We have also corrected a typo in the csch-term.

B Additional ISZ energy spectra

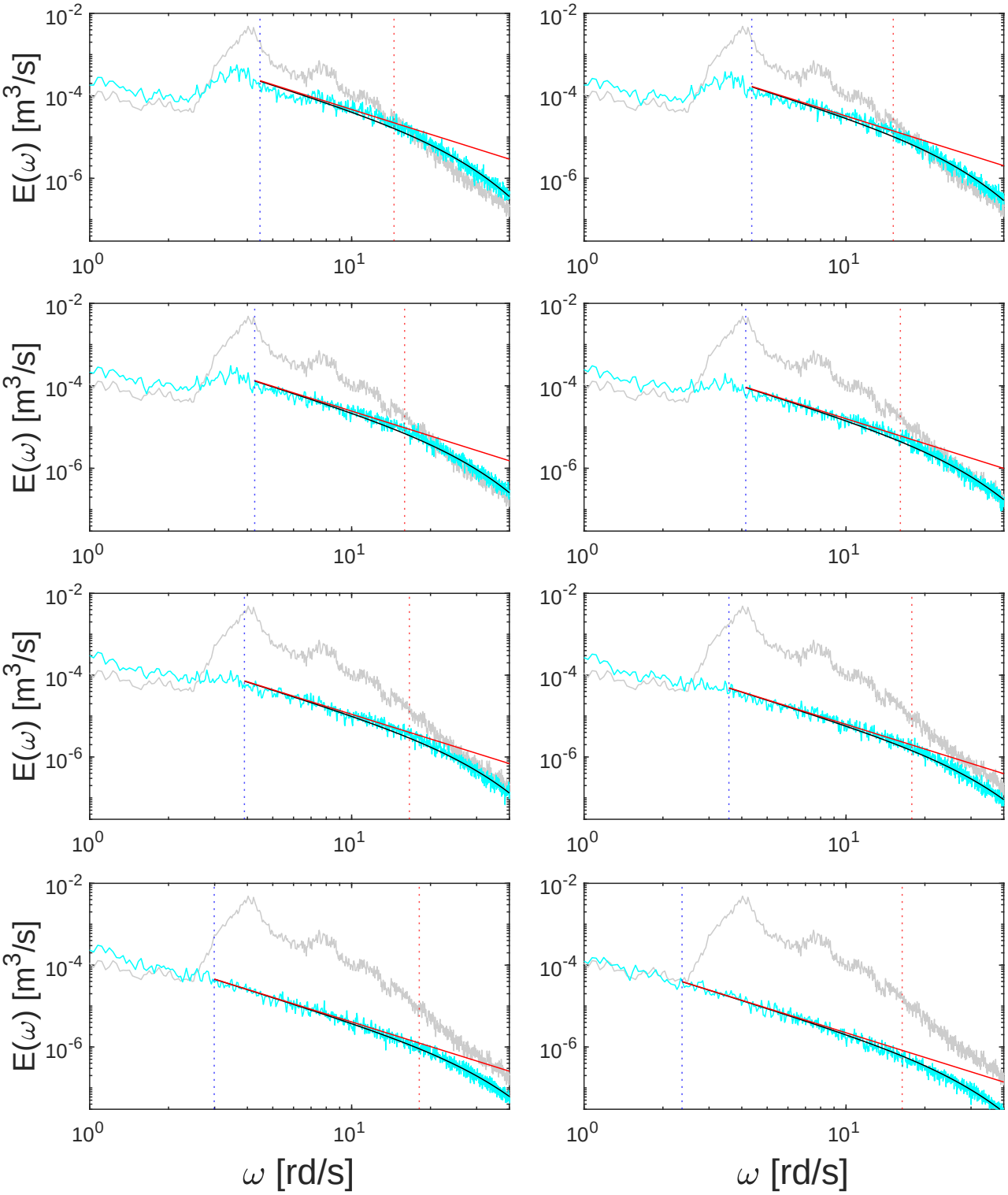

Figure 3: Energy spectra at different locations in the ISZ for the vN03-D3 experiment. a, gauge 62, $h_0 = 6.8$ cm; b, gauge 63, $h_0 = 6.0$ cm; c, gauge 64, $h_0 = 5.2$ cm; d, gauge 65, $h_0 = 4.4$ cm; e, gauge 66, $h_0 = 3.6$ cm; f, gauge 67, $h_0 = 2.9$ cm. Grey line, spectrum at the breaking point; cyan line, ISZ spectrum at water depth h_0; black line, equation (23); red line, equation (24). Blue dashed line, position of ω_m; red dashed line, position of ω_ν.

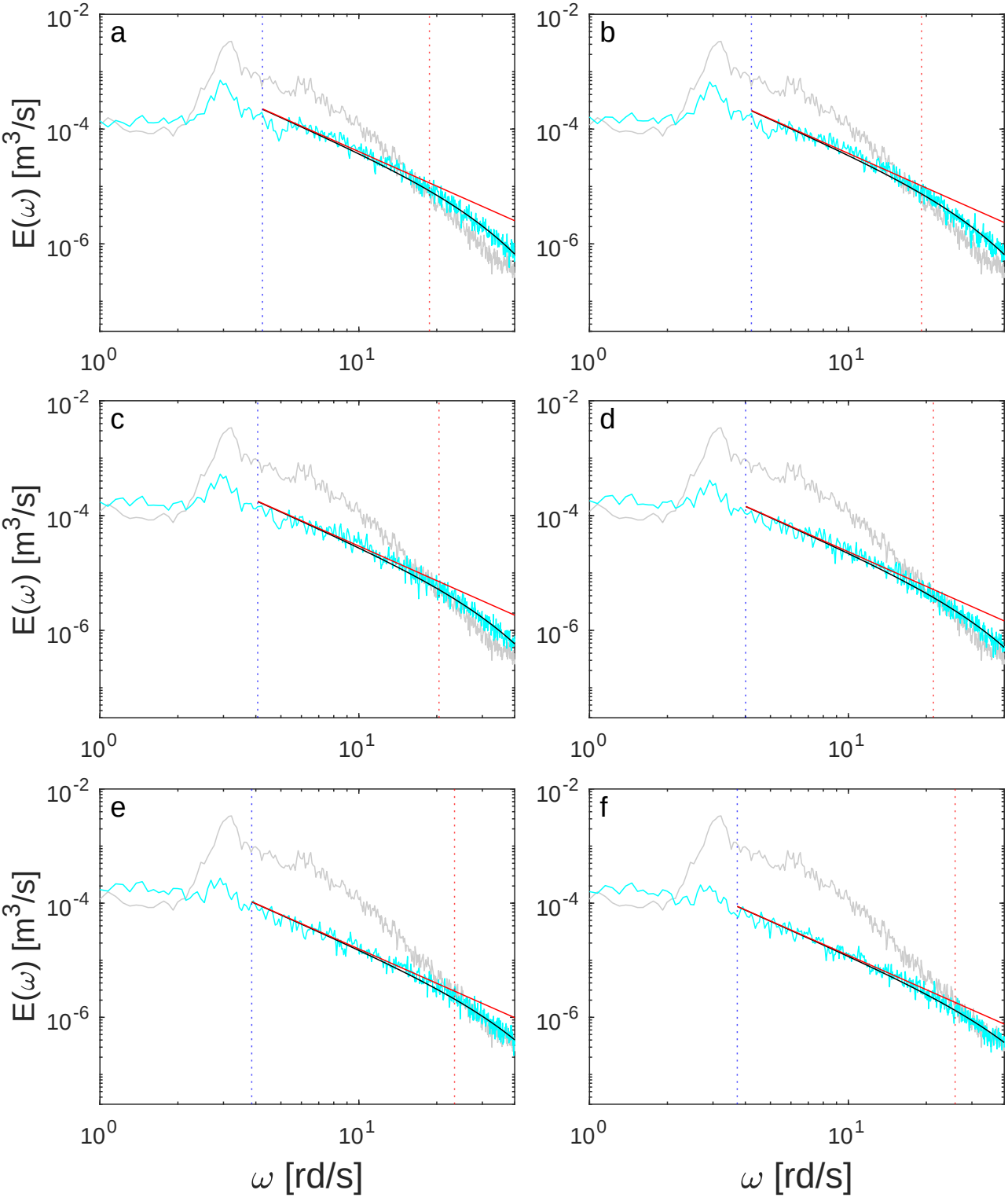

Figure 4: Energy spectra at different locations in the ISZ for the BK94-7 experiment. a, $x = 24.50$ m, $h_0 = 7.4$ cm; b, $x = 24.72$ m, $h_0 = 6.7$ cm; c, $x = 24.97$ m, $h_0 = 6.0$ cm; d, $x = 25.22$ m, $h_0 = 5.3$ cm; e, $x = 25.50$ m, $h_0 = 4.6$ cm; f, $x = 25.76$ m, $h_0 = 3.8$ cm. Grey line, spectrum at the breaking point; cyan line, ISZ spectrum at water depth h_0; black line, equation (23); red line, equation (24). Blue dashed line, position of ω_m; red dashed line, position of ω_ν.

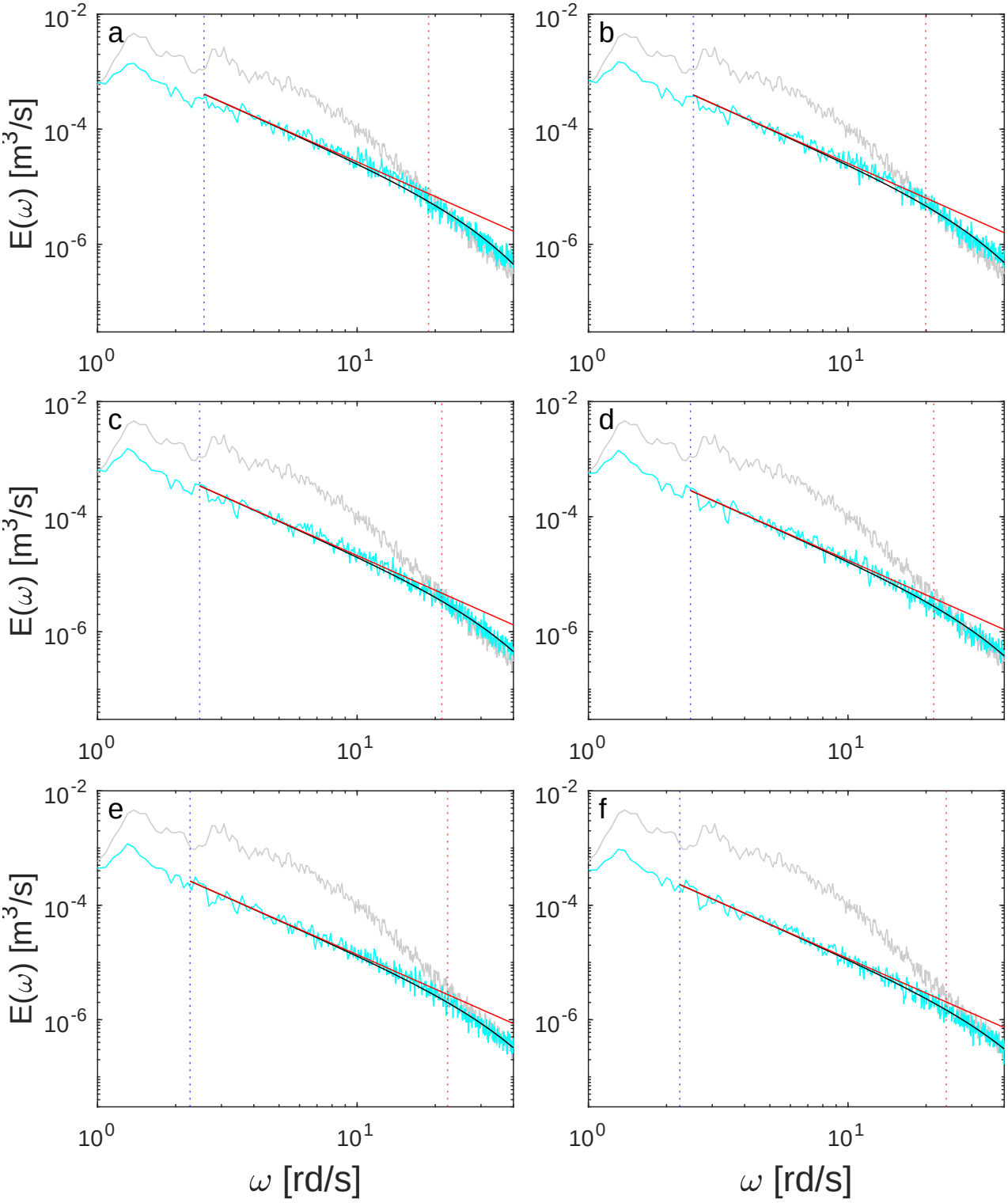

Figure 5: Energy spectra at different locations in the ISZ for the BK94-8 experiment. a, $x = 24.50$ m, $h_0 = 7.5$ cm; b, $x = 24.72$ m, $h_0 = 6.8$ cm; c, $x = 24.97$ m, $h_0 = 6.1$ cm; d, $x = 25.22$ m, $h_0 = 5.5$ cm; e, $x = 25.50$ m, $h_0 = 4.8$ cm; f, $x = 25.76$ m, $h_0 = 3.9$ cm. Grey line, spectrum at the breaking point; cyan line, ISZ spectrum at water depth h_0; black line, equation (23); red line, equation (24). Blue dashed line, position of ω_m; red dashed line, position of ω_ν.

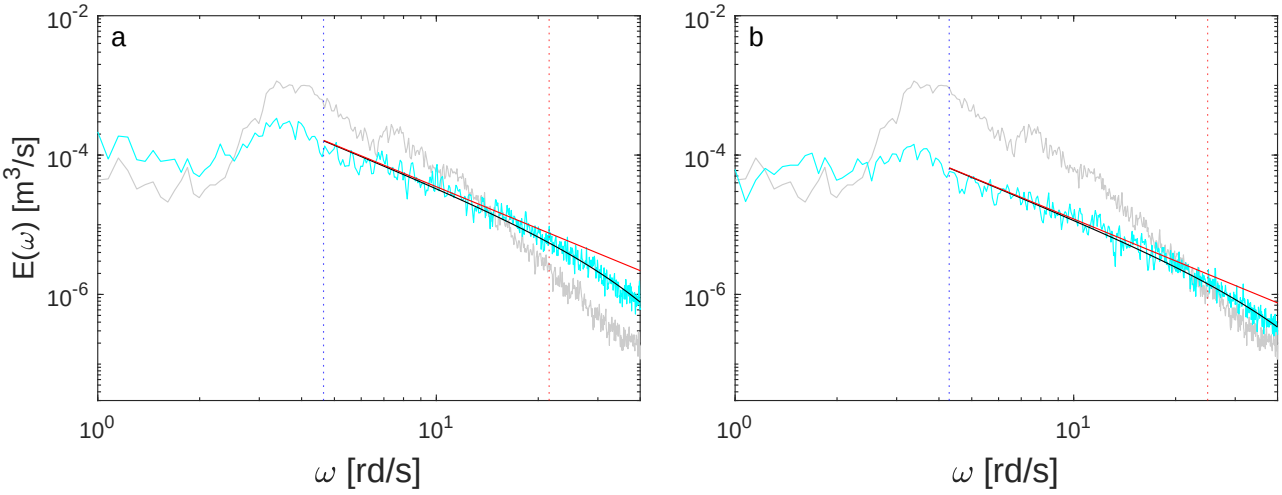

Figure 6: Energy spectra at 2 locations in the ISZ for the MK93 experiment. a, gauge 10, $h_0 = 5.3$ cm; b, gauge 11, $h_0 = 3.5$ cm. Grey line, spectrum at the breaking point; cyan line, ISZ spectrum at water depth h_0; black line, equation (23); red line, equation (24). Blue dashed line, position of ω_m; red dashed line, position of ω_ν.

References

Gurbatov, S. N., Rudenko, O. V., and Saichev, A. I. (2012). Waves and structures in nonlinear nondispersive media: general theory and applications to nonlinear acoustics. *Springer Science & Business Media*.

Oberhettinger, F. (1957). Tabellen zur Fourier transformation. Springer-Verlag.

Saffman, P. G. (1968). Lectures on homogeneous turbulence. *Topics in nonlinear physics*, ed. N.J. Zabusky. New York: Springer, 485-614.